

0017-9310(94)00230-4

# The prediction of the critical heat flux in water-subcooled flow boiling

G. P. CELATA, M. CUMO, A. MARIANI and G. ZUMMO

ENEA–Energy Department, C.R.E. Casaccia, Via Anguillarese 301, 00060 Rome, Italy

(Received 17 March 1994 and in final form 14 June 1994)

**Abstract**—The prediction of water-subcooled flow boiling critical heat flux (CHF) in peripherally non-uniform heated tubes with or without swirl flow promoters is accomplished using a model based on the liquid sublayer dryout mechanism recently proposed by the authors. Peripheral nonuniform heating and/or twisted-tape inserts are properly and simply accounted for in the model, originally developed for uniform heating and straight flow. Simultaneous occurrence of the two events is also well predicted by the model. Although initially formulated for operating conditions typical of the thermal hydraulic design of fusion reactor high heat flux components, the model is proved to give a satisfactory answer for the prediction of the CHF under more general conditions, provided local thermodynamic conditions of the bulk flow at the CHF are sufficiently far from the saturated state.

## 1. INTRODUCTION

The critical heat flux (CHF) in water-subcooled flow boiling has been extensively investigated in the past with particular reference to the thermal hydraulic design of light water reactors [1–3]. Recently, cooling requirements of high heat flux components in thermonuclear fusion reactors called for the CHF in water-subcooled flow boiling to be studied under conditions of very high mass flux and subcooling. In fact, the above thermal hydraulic conditions, coupled with relatively small tube diameters, allow very high values of the CHF to be reached, up to some tens of MW m<sup>-2</sup>. A very recent state-of-the-art review has been proposed by Celata [4].

A model for the prediction of the CHF in water-subcooled flow boiling under conditions of very high mass flux and liquid subcooling and low/medium pressure for a uniformly heated tube, has been recently proposed by Celata *et al.* [5]. The aim of the present paper is: (i) to ascertain the possibility of predicting more complex situations, such as the circumferential non-uniform heating and the presence of swirl flow promoters (twisted tapes) to enhance the CHF; (ii) to present the performances of the above model in predicting the subcooled flow boiling CHF under thermal hydraulic conditions of low/medium mass flux and high pressure to extend its validity.

## 2. THE SUBCOOLED FLOW BOILING CHF MODEL

The model described in ref. [5] is based on the liquid sublayer dryout mechanism, starting from the observation that, during fully developed boiling, a vapour blanket forms in the vicinity of the heated wall by the coalescence of small bubbles, leaving a thin

liquid sublayer in contact with the heated wall beneath the blanket. The CHF is assumed to occur when the liquid sublayer is extinguished by evaporation during the passage time of the vapour blanket.

Parameters to be determined are: initial thickness of the liquid sublayer  $\delta$ , vapour blanket length  $L_B$ , and velocity  $U_B$ . The evaluation of  $\delta$  is obtained from the following argument. Vapour blanket can develop and exist only in the near-wall region, where the local liquid temperature is greater or equal to the saturation value. Considering the temperature distribution from the heated wall to the centre of the channel, it will exist a distance from the wall at which the temperature is equal to the saturation value at the local pressure. This distance defines the 'superheated layer', and is indicated with  $y^*$ . For a distance from the wall greater than  $y^*$ , the blanket (and each single bubble) will collapse in the subcooled liquid bulk. Considering also that the vapour blanket is pushed toward the centre of the tube by the velocity gradient, it is assumed that the vapour blanket location in the superheated layer is such to occupy the region closer to the saturation limit, i.e. as far as possible from the heated wall, but within the superheated layer,  $y^*$ . The liquid sublayer thickness,  $\delta$ , can therefore be calculated as the difference between the superheated layer,  $y^*$ , and the vapour blanket thickness,  $D_B$ . Vapour blanket length  $L_B$ , is postulated to be equal to the critical wavelength of Helmholtz instability at the liquid–vapour interface. Vapour blanket velocity,  $U_B$ , is obtained by superimposing the liquid velocity, calculated using the Karman velocity distribution and the relative blanket velocity, with respect to the liquid, deduced from a forces balance applied to the vapour blanket (buoyancy and drag forces). Referring the reader to ref. [5] for details, equations used in the model for the calculation of the CHF are summarized in Table 1.

## NOMENCLATURE

$C_D$	drag coefficient, dimensionless	$y^+$	non-dimensional distance from the heated wall.
CHF	critical heat flux [ $\text{W m}^{-2}$ ]	<b>Greek symbols</b>	
$C_p$	specific heat at constant pressure [ $\text{J kg}^{-1} \text{K}^{-1}$ ]	$\beta$	contact angle, dimensionless
$D$	diameter [m]	$\delta$	liquid sublayer initial thickness [m]
$f$	friction factor, dimensionless	$\Gamma$	mass flow rate [ $\text{kg s}^{-1}$ ]
$f_{tt}$	twisted-tape friction factor, given by equation (1), dimensionless	$\gamma$	twist tape ratio, the number of tube diameters per $180^\circ$ twist in the tape, dimensionless
$f(\beta)$	function of contact angle, 0.02–0.03, dimensionless	$\phi$	angle, dimensionless
$G$	mass flux [ $\text{kg m}^{-2} \text{s}^{-1}$ ]	$\lambda$	latent heat of vaporization [ $\text{J kg}^{-1}$ ]
$g$	gravitational acceleration [ $\text{m s}^{-2}$ ]	$\mu$	dynamic viscosity [ $\text{kg s}^{-1} \text{m}^{-1}$ ]
$K$	thermal conductivity [ $\text{W m}^{-1} \text{K}^{-1}$ ]	$\nu$	cinematic viscosity [ $\text{m}^2 \text{s}^{-1}$ ]
$L$	length [m]	$\rho$	density [ $\text{kg m}^{-3}$ ]
$p$	pressure [MPa]	$\sigma$	surface tension [ $\text{N m}^{-1}$ ]
$Pr$	Prandtl number: $C_p \mu / K$ , dimensionless	$\tau_w$	wall shear stress [MPa].
$Q$	$q'' / \rho_L C_{pL} U_\tau$ [ $^\circ\text{C}$ ]	<b>Subscripts</b>	
$q''$	heat flux [ $\text{W m}^{-2}$ ]	B	pertains to the vapour blanket
$R$	channel radius [m]	in	inlet
$Re$	Reynolds number: $GD/\mu$ , dimensionless	L	pertains to the liquid phase
$S$	heat transfer surface [ $\text{m}^2$ ]	m	mean
$T$	temperature [ $^\circ\text{C}$ ]	max	maximum
$U$	velocity [ $\text{m s}^{-1}$ ]	min	minimum
$U_\tau$	friction velocity: $(\tau_w/\rho_L)^{0.5}$ [ $\text{m s}^{-1}$ ]	out	exit conditions
$x$	steam quality, dimensionless	sat	pertains to saturated conditions
$y$	distance from the heated wall [m]	sub	pertains to subcooled conditions
$y^*$	superheated layer thickness [m]	v	pertains to the vapour phase
		w	pertains to the wall.

Physical properties are calculated at saturated state at the exit pressure, except for  $C_{pL}$  in the coolant heat balance, calculated at the average coolant temperature along the channel,  $(T_m + T_{in})/2$ . The heat flux at the wall is supposed to be uniform both along the axis and the circumference of the tube.

### 3. PERIPHERAL NON-UNIFORM HEATING

The effect of non-uniform heating along the circumference of the tube is of relevant importance in the thermal hydraulic design of fusion reactors high heat flux components. In fact, as an example, the divertor is thermally loaded only on one side.

*Ad hoc* experiments were recently carried out by Nariai *et al.* [10] and by Gaspari [11]. In particular, Gaspari gave a comparison between peripherally full and half-heated tubes, straight flow, analyzing the CHF at both inlet and exit thermal hydraulic conditions. Using a 10 mm i.d. channel, 0.15 m long, Gaspari observed that, under constant inlet liquid subcooling, higher CHF values were observed for half-heated tubes. Plotting the CHF vs exit liquid subcooling, such differences tend to disappear. This experimental evidence is reported in Fig. 1, where the

CHF is plotted vs inlet/outlet subcooling. It shows that the influence of the channel heating on the boiling crisis (circumferentially uniform or non-uniform heating) may be neglected once the CHF is referred to local conditions. The latter is a further confirmation that the boiling crisis in subcooled flow boiling can be regarded as a local phenomenon. In Nariai *et al.* [10] the non-uniform heating is such that the heat flux is higher over  $180^\circ$  or  $270^\circ$  and lower over  $180^\circ$  or  $90^\circ$ , respectively, being different from zero in the latter regions (thinned part of the tube). Figure 2 shows a schematic of the Nariai *et al.* [10] and Gaspari [11] experiments.

Circumferential non-uniform heating can be accounted for in the model description, simply by changing the heat flux,  $q''$ , in the coolant heat balance for the calculation of the exit average coolant temperature,  $T_m$ . In particular, we have to use the average heat flux, equal to  $0.5q''$  in the Gaspari experiments [11] (where  $q''$  is the heat flux in the half-heated part of the tube), and  $0.5(q''_{\max} + q''_{\min})$  for  $\phi = 180^\circ$  tests, and  $0.75q''_{\max} + 0.25q''_{\min}$  for  $\phi = 270^\circ$  tests in the Nariai *et al.* experiments [10] (where  $q''_{\max} + q''_{\min}$  are the higher and the lower heat flux, respectively). It is evident that the exit bulk thermal hydraulic conditions, which the

Table 1. Equations for the numerical iteration of CHF

- Wall temperature,  $T_w$  (obtained by equating the liquid average temperature given by the coolant heat balance and the radial temperature distribution in the liquid [6])

$$T_w = T_m + \frac{5Q}{y^+(R)} \left\{ Pr \left[ \frac{2y^+(R) - 5}{2} \right] + \frac{5}{Pr} [(1 + 5Pr) (\ln(1 + 5Pr) - 1) + 1] \right. \\ \left. + \ln(1 + 5Pr)[y^+(R) - 30] + \frac{y^+(R) \left[ \ln \left( \frac{y^+(R)}{30} \right) - 1 \right] + 30}{2} \right\}$$

$$T_m = T_{in} + \frac{q'' S}{\Gamma C_{pL}} \quad Q = \frac{q''}{\rho_L C_{pL} U_\tau} \quad U_\tau = \frac{G}{\rho_L} \sqrt{\frac{f}{8}} \quad y^+ = \frac{y}{\nu_L} U_\tau.$$

- Bubble diameter,  $D_B$  [7]

$$D_B = \frac{32}{f} \frac{\sigma f(\beta) \rho_L}{G^2} \quad f(\beta) = 0.03.$$

- Friction factor,  $f$  [8]

$$\frac{1}{\sqrt{f}} = 1.14 - 2.0 \log \left( \frac{0.72 \sigma \rho_L}{f D G^2} + \frac{9.35}{Re \sqrt{f}} \right).$$

- Initial sublayer thickness,  $\delta$

$$\delta = y^* - D_B$$

where  $y^*$  is the distance from the wall for which  $T(y^*) = T_{sat}$ , using the temperature distribution given by Martinelli [6].

- Blanket velocity,  $U_B$  (from the Karman velocity distribution)

$$U_B = \left( \frac{2L_B g(\rho_L - \rho_V)}{\rho_L C_D} \right)^{0.5} + 0.125 \left( \delta + \frac{D_B}{2} \right) \frac{f G^2}{\rho_L \mu_L} \quad 0 \leq y^+ < 5 \\ U_B = \left( \frac{2L_B g(\rho_L - \rho_V)}{\rho_L C_D} \right)^{0.5} + 1.768 \sqrt{f} \frac{G}{\rho_L} \left\{ \ln \left[ 0.354 \frac{G}{\mu_L} \sqrt{f} \left( \delta + \frac{D_B}{2} \right) \right] - 0.61 \right\} \quad 5 \leq y^+ < 30 \\ U_B = \left( \frac{2L_B g(\rho_L - \rho_V)}{\rho_L C_D} \right)^{0.5} + 0.884 \sqrt{f} \frac{G}{\rho_L} \left\{ \ln \left[ 0.354 \frac{G}{\mu_L} \sqrt{f} \left( \delta + \frac{D_B}{2} \right) \right] + 2.2 \right\} \quad y^+ \geq 30.$$

- Drag coefficient,  $C_D$  [9]

$$C_D = \frac{2}{3} \frac{D_B}{\left( \frac{\sigma}{g(\rho_L - \rho_V)} \right)^{0.5}}$$

- Blanket length,  $L_B$

$$L_B = \frac{2\pi\sigma(\rho_V + \rho_L)}{\rho_V \rho_L U_B^2}.$$

- Critical heat flux,  $q''_{CHF}$

$$q''_{CHF} = \frac{\rho_L \delta \lambda}{L_B} U_B$$

CHF is strongly dependent on [4], are only a function of the average heat flux (i.e. the total thermal power delivered to the fluid), independent of its distribution.

As a boiling crisis in subcooled flow boiling is a strictly local phenomenon, all equations employed in the model mathematical description can be used also in the case of peripheral non-uniform heating. In fact, all calculations, except for  $T_m$ , are made using the maximum value of the heat flux, and all parameters used to calculate the CHF are local values:  $\delta$ ,  $U_B$ ,  $L_B$ ,

$T_w$ ,  $D_B$ ,  $y^*$ . Temperature and velocity distributions are still valid in the sector interested by the heat flux, as in the Gaspari experiments [11], or the highest heat flux, as in the Nariai *et al.* experiments [10]. A possible distortion of such distributions is likely to happen in the bulk of the flow, due to turbulent mixing. As velocity and temperature distributions are used locally in the calculation of the CHF ( $y^*$  is of the order of magnitude of some tens of microns), it looks reasonable to continue to make use of such distributions

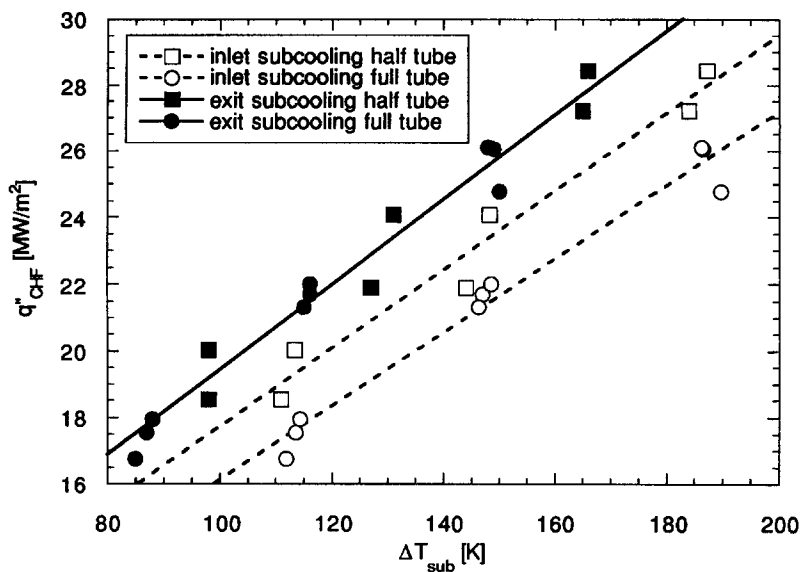


Fig. 1. Influence of peripheral non-uniform heating on CHF. Analysis at local and inlet conditions [11].

in the case of peripheral non-uniform heating. The prediction of the few experimental data obtained by Nariai *et al.* [10] using the Celata *et al.* model [5] is

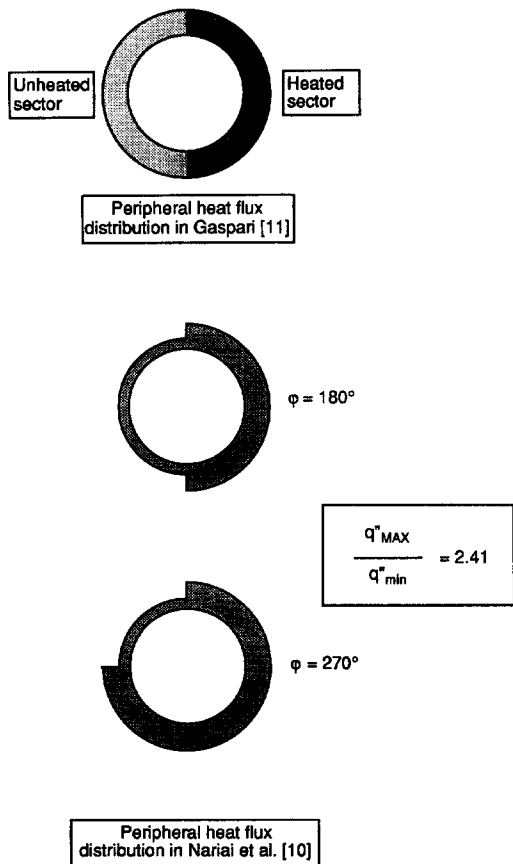


Fig. 2. Schematic of peripheral non-uniform heating in Gaspari [11] and Nariai *et al.* [10].

shown in Fig. 3, where the ratio between the calculated and the experimental critical heat flux is plotted vs the exit quality,  $x_{out}$ . The agreement is generally good, independent of the two different heating non-uniformities investigated. There is a tendency to underestimate the CHF as exit thermal hydraulic conditions approach the bulk saturation ones. The prediction of the Gaspari data [11] is shown in Fig. 4, in a similar representation as the previous figure. The agreement is also good in this case, most of the 26 experimental data being within  $\pm 20\%$ . The maximum value of the exit quality in the Gaspari data is lower than in the Nariai *et al.* data. Therefore, the systematic effect observed in Fig. 3 as  $x_{out}$  tends to zero is not evident in the Gaspari data prediction.

4. PRESENCE OF SWIRL FLOW PROMOTERS

Although high heat fluxes, such as those requested for fusion reactor applications, could be physically obtained using water-subcooled flow boiling in straight tubes, nonetheless engineering considerations that limit the variation of parameters such as velocity, channel diameter and liquid subcooling, and safety margins, called for the employment of suitable techniques to further enhance the upper limit of the heat transfer, i.e. the CHF.

Recent experiments showed that use of twisted tapes as swirl flow promoters in water-subcooled flow boiling is very effective in CHF enhancement, allowing increases in the CHF up to a factor of 2.0 [12, 13].

The Celata *et al.* model [5] may be used to predict CHF swirl flow data, making use of same corrections already used in empirical correlations. As the presence of a twisted tape inside a channel is associated with a relevant increase in the pressure drop (e.g. up to a

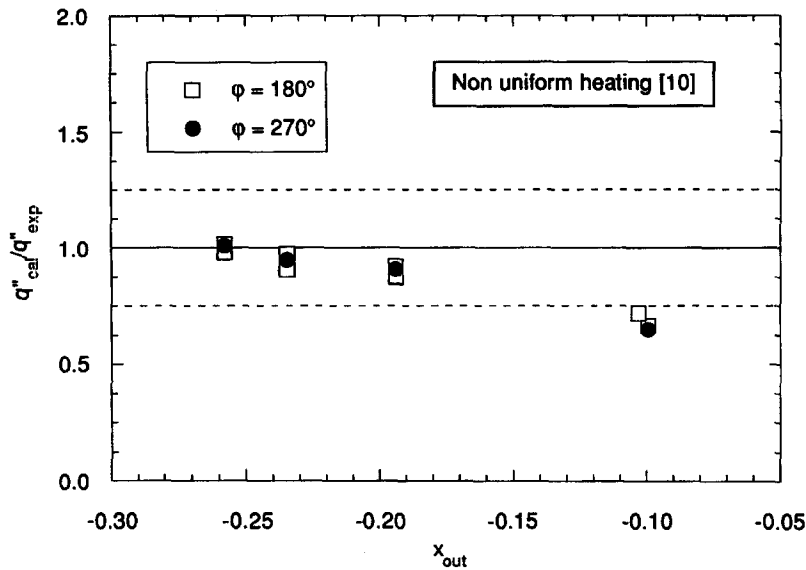


Fig. 3. Prediction of peripheral non-uniform heating, straight flow CHF data [10].

factor of 11 in ref. [13]), a friction factor correction for twisted tapes was suggested by Lopina and Bergles [14]. Based on experiments, Lopina and Bergles show that the friction factor,  $f_{tt}$ , for use in the twisted tape geometry varies as

$$f_{tt} = 2.75f\gamma^{-0.406} \quad (1)$$

where  $\gamma$  is the twist ratio of the tape, a measure of the number of tube diameters per  $180^\circ$  twist in the tape, and  $f$  is the friction factor for straight tube. More recently, Koski [15] showed that, in the case of very high heat fluxes, the constant 2.75 should be replaced

with 2.2. To extend the Celata *et al.* model [5] for use with twisted tapes, equation (1) was tried.

The prediction of the Nariai *et al.* data [12] is shown in Fig. 5, where the ratio between the calculated and the experimental CHF is plotted vs exit quality,  $x_{out}$ . The agreement is quite encouraging, as almost all the data are predicted within  $\pm 25\%$ , showing that the procedure can be successful.

Recent experiments by Cardella *et al.* [13] were carried out with twisted tapes inserted in peripherally half-heated tubes. In addition to the above correction for twisted tapes, the Celata *et al.* model was used as

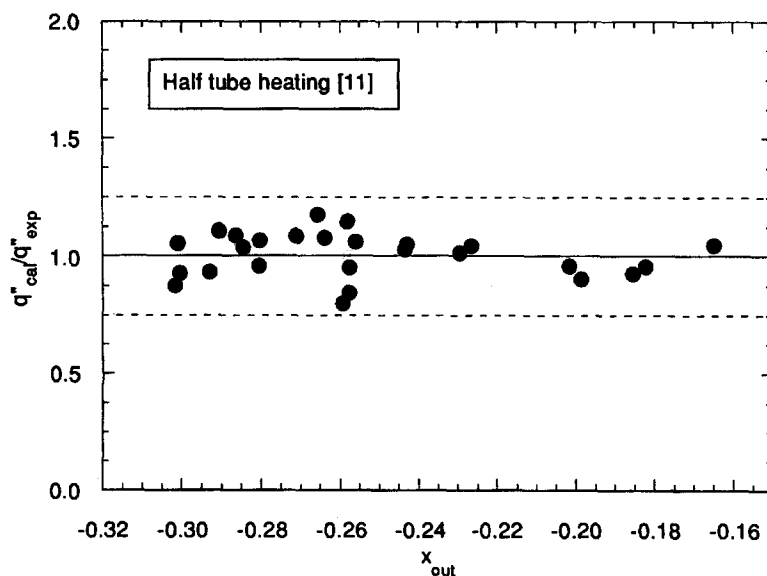


Fig. 4. Prediction of peripheral non-uniform heating, straight flow CHF data [11].

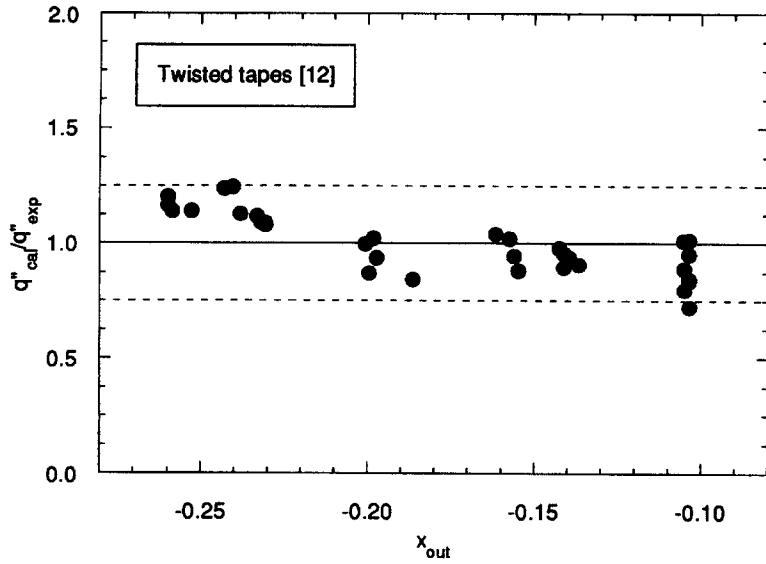


Fig. 5. Prediction of swirl flow CHF data [12].

described in Section 3. The results of the prediction are shown in Fig. 6, similarly to Fig. 5. The agreement can be considered satisfactory in view of the complexity of the situation in comparison with the original description of the model. Although a general underestimation of the CHF is observed, most of the experimental data are predicted within  $\pm 25\%$ .

The use of the Koski recommended constant [15] for equation (1) did not make any difference in the above calculations.

#### 5. LOW MASS FLUX-HIGH PRESSURE DATA

Although the Celata *et al.* model [5] is developed for high mass flux, high liquid subcooling and low/medium pressure conditions, it is of interest to verify its validity under different operating conditions, provided exit subcooled conditions still exist. As is known, subcooled flow boiling CHF was studied in the past with reference to pressurized water reactors, i.e. low mass flux, high pressure and low liquid sub-

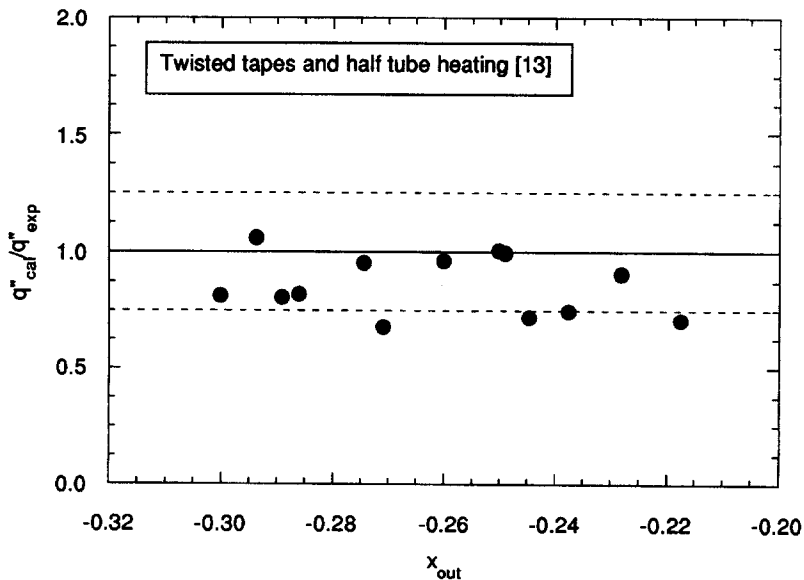


Fig. 6. Prediction of swirl flow, peripheral non-uniform heating CHF data [13].

cooling (collections of data are reported in refs. [16–18]). The assumptions which the Celata *et al.* model are based on rely on the hypothesis that the mass flux is sufficiently high (greater than 2000–3000 kg m<sup>-2</sup> s<sup>-1</sup>) and exit thermal hydraulic conditions are not very close to the saturation ones (let us say  $x_{out} < -0.1$ ). It is evident that a mass flux lower than the above limits may worsen the performances of the model, reducing its capability to predict the CHF in subcooled flow boiling to  $x_{out} < -0.2$  or less. The prediction of the experimental data gathered in refs. [16–18] is shown in Fig. 7, where, as usual, the calculated-to-experimental CHF ratio is plotted vs exit quality,  $x_{out}$ . Low mass flux stands for  $G < 3000$  kg m<sup>-2</sup> s<sup>-1</sup>, and low pressure stands for  $p < 8.0$  MPa. The overall operating ranges of such data are as follows:  $350 < G < 18\,600$  kg m<sup>-2</sup> s<sup>-1</sup>,  $1.38 < p < 20.7$  MPa,  $1.14 < D < 37.5$  mm,  $11.7 < L/D < 365.3$ ,  $-0.664 < x_{out} < -0.044$ ,  $1.1 < CHF < 21.4$  MW m<sup>-2</sup>.

The performance of the model with the above data is as expected. A reasonable agreement with experimental data is shown as long as exit thermodynamic conditions are not so close to the saturated state. The threshold in terms of  $x_{out}$  depends on mass flux and ranges from  $x_{out} = -0.2$  (very low mass flux) to  $x_{out} = -0.1$  (low mass flux). As already anticipated, predictions of low mass flux data are worse than those of high mass flux data, even at reasonably high exit subcooling ( $x_{out} < -0.3$ ). Plotting the ratio between calculated and experimental CHF vs inlet subcooling, as shown in Fig. 8, it is interesting to observe that, for liquid subcooling,  $\Delta T_{sub,in}$ , lower than 50 K, experimental data are very underestimated, independent of either  $G$  or  $p$ .

In order to make a quick correspondence between exit quality,  $x_{out}$ , and exit subcooling,  $\Delta T_{sub,out}$ , depending on the pressure, the functional dependence

is shown in Fig. 9, where  $x_{out}$  is plotted vs  $\Delta T_{sub,out}$ , for different values of the pressure (local value).

## 6. CONCLUDING REMARKS

A newly developed model for the prediction of the CHF in water subcooled flow boiling has been recently proposed by Celata *et al.* [5]. It is based on the liquid sublayer dryout mechanisms, and is specifically thought to predict the CHF under conditions of high mass flux ( $G$  up to 90 Mg m<sup>-2</sup> s<sup>-1</sup>), intermediate-to-low pressure ( $p < 8.4$  MPa), high liquid subcooling (up to 255 K), typical of the thermal hydraulic design of high heat flux components in fusion reactors [4]. The model is developed for peripheral uniform heating and smooth flow in the channel.

Nonetheless, peripheral non-uniform heating is typical of some high heat flux components (i.e. the divertor), and the use of twisted tapes as swirl flow promoters for the CHF enhancement is pursued. The Celata *et al.* model may easily account for the two above situations (also simultaneously occurring) by:

- considering the total thermal power delivered to the fluid in the coolant heat balance for the calculation of local thermal hydraulic conditions;
- modifying the friction factor for straight flow to take into consideration the relevant pressure drop increase due to inserted swirl flow promoters (corrections suggested by Lopina and Bergles [14] and by Koski [15] were used).

With the above considerations, the Celata *et al.* model shows a good capability to predict CHF experimental data carried out with peripheral non-uniform heating and/or swirl flow promoter inserts, i.e. fusion reactor-relevant data, resulting a suitable tool for the thermal

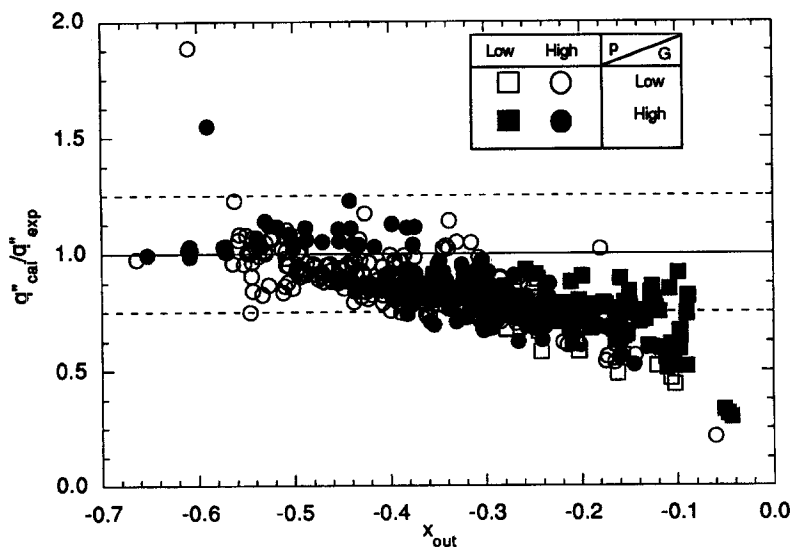


Fig. 7. Prediction of CHF data gathered in refs. [16–18]: calculated-to-experimental CHF vs exit quality.

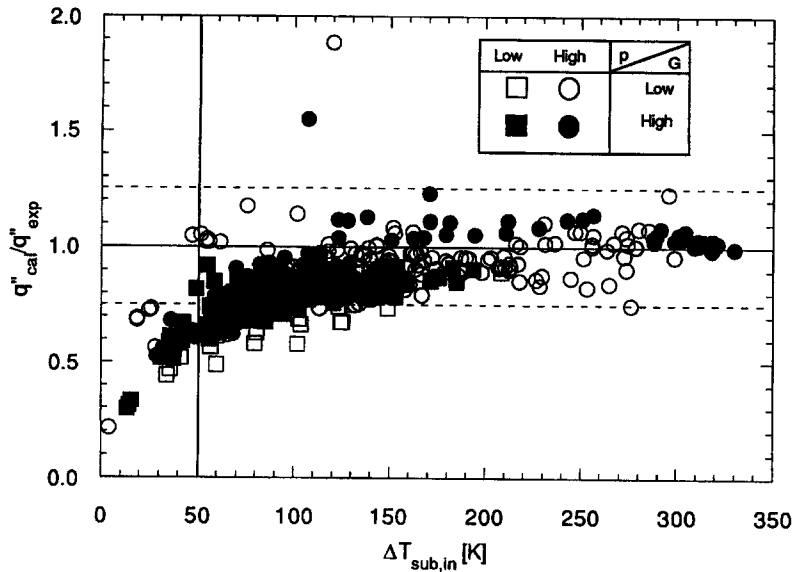


Fig. 8. Prediction of CHF data gathered in refs. [16–18]: calculated-to-experimental CHF vs inlet subcooling.

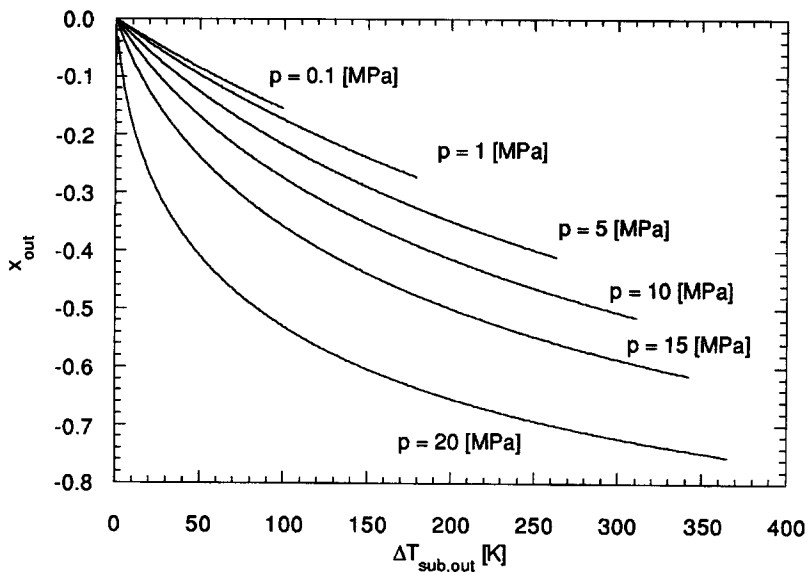


Fig. 9. Exit quality vs exit subcooling as a function of the exit pressure.

hydraulic design of fusion reactor high heat flux components.

Looking through the mathematical description of the model, one may realize that the model could also be extended to conditions different from those which it was originally formulated on, provided bulk subcooled conditions at the CHF location are guaranteed. To verify the validity bounds of the model and to categorize its presumed general validity, a test has been conducted using experimental data essentially carried out under typical pressurized water reactor operating conditions [16–18], i.e. high pressure, low mass flux, intermediate-to-low liquid subcooling.

The performances of the model can be considered

satisfactory up to exit qualities between  $-0.2$  and  $-0.1$ , depending upon mass flux. It loses its validity when local thermodynamic conditions at the CHF approach the saturated state of the bulk, and when the mass flux is relatively low (less than  $1000\text{--}2000$   $\text{kg m}^{-2} \text{s}^{-1}$ ). General validity of the model for the prediction of the CHF under subcooled flow boiling conditions is substantially obtained, and validity bounds are also provided.

*Acknowledgements*—Authors are deeply grateful to Professor Y. Katto for the very fruitful discussions, and to Dr S. T. Yin, who provided many of the experimental data used in the present study. Thanks are due to Mrs A. M. Moroni who took care of the general editing of the paper.



## REFERENCES

1. A. E. Bergles, J. G. Collier, J. M. Delhaye, G. F. Hewitt and F. Mayinger, *Two-phase Flow and Heat Transfer in the Power and Process Industries*, pp. 226–255. Hemisphere, New York (1981).
2. J. G. Collier, *Convective Boiling and Condensation* (2nd Edn), pp. 144–177. McGraw-Hill, New York (1981).
3. Y. Y. Hsu and R. W. Graham, *Transport Processes in Boiling and Two-phase Systems*, pp. 217–232. American Nuclear Society (1986).
4. G. P. Celata, Recent achievements in the thermal hydraulics of high heat flux components in fusion reactors, *Expl Therm. Fluid Sci.* **7**, 177–192 (1992).
5. G. P. Celata, M. Cumo, A. Mariani, M. Simoncini and G. Zummo, Rationalization of existing mechanistic models for the prediction of water subcooled flow boiling critical heat flux, *Int. J. Heat Mass Transfer* **37**, Suppl. 1, 347–360 (1994).
6. R. C. Martinelli, Heat transfer to molten metals, *Trans. ASME* **69**, 947–951 (1947).
7. F. W. Staub, The void fraction in subcooled boiling—prediction of the initial point of net vapour generation, *J. Heat Transfer* **90**, 151–157 (1968).
8. S. Levy, Forced convection subcooled boiling—prediction of vapour volumetric fraction, *Int. J. Heat Mass Transfer* **10**, 951–965 (1967).
9. T. Z. Harmathy, Velocity of large drops and bubbles in media of infinite and restricted extent, *A.I.Ch.E. JI* **6**, 281–288 (1960).
10. H. Nariyai, F. Inasaka, A. Ishikawa and W. Fujisaki, Critical heat flux of subcooled flow boiling in tube with internal twisted tape under non-uniform heating conditions, *Proceedings of the 2nd JSME-KSME Thermal Engineering Conference*, Vol. 3, pp. 285–288 (1992).
11. G. P. Gaspari, Comparison among data of electrically and e-beam heated tubes, *Proceedings of the 3rd International Workshop on High Heat Flux Components Thermal Hydraulics in Fusion Reactors*, Cadarache (1993).
12. H. Nariyai, F. Inasaka, W. Fujisaki and H. Ishiguro, Critical heat flux of subcooled flow boiling in tubes with internal twisted tapes, *Proceedings of the ANS Winter Meeting (THD)*, pp. 38–46 (1991).
13. A. Cardella, G. P. Celata, G. Dell'Orco, G. Gaspari, G. Cattadori and A. Mariani, Thermal hydraulics experiments for the NET divertor, *Proceedings of the 17th Symposium on Fusion Technology*, Vol. 1, pp. 206–210 (1992).
14. R. F. Lopina and A. E. Bergles, Heat transfer and pressure drop in tape-generated swirl flow of single-phase water, *J. Heat Transfer* **91**, 8–13 (1969).
15. J. A. Koski, Thermal-hydraulic considerations in the surface contouring of a limiter head for Tore Supra, *Proceedings of the ANS Winter Meeting (THD)*, pp. 7–17 (1991).
16. C. L. Williams and S. G. Beus, Critical heat flux experiments in a circular tube with heavy water and light water, Westinghouse Report, WAPD-TM-1462 (1980).
17. J. M. Robertson, Heat transfer to high pressure steam water mixtures, HTFS Report, HTFS-DR 6 (AERE-R 6189), Commercial in Confidence (1971).
18. B. Thompson and R. V. Macbeth, Boiling water heat transfer—burnout in uniformly heated round tubes: a compilation of world data with accurate correlations, AEEW-R 356 (1964).